Cerebral Cortex February 2015;25:528–537
doi:10.1093/cercor/bht252
Advance Access publication September 17, 2013

Haptic Working Memory for Grasping: the Role of the Parietal Operculum

Francesca Maule[1], Guido Barchiesi[1], Thomas Brochier[2] and Luigi Cattaneo[1]

[1]Center for Mind/Brain Sciences (CIMeC), University of Trento, Italy, [2]INT, CNRS-Aix-Marseille Université, Marseille, France

Address correspondence to Dr Luigi Cattaneo, Center for Mind/Brain Sciences (CIMeC), University of Trento, Via delle Regole, 101, I - 38123 Mattarello, TN, Italy. Email: luigi.cattaneo@unitn.it

We investigated how haptic information on object geometry is encoded in the parietal operculum (OP) and is used for guiding object-directed motor acts in humans. We tested the effects of conditioning single-pulse transcranial magnetic stimulation (spTMS) applied to the left OP on corticospinal excitability assessed by a test spTMS applied to the ipsilateral motor cortex (M1) 5 ms after conditioning spTMS. Participants explored the size of a graspable object visually or haptically and waited for a go-signal to grasp it in the dark. They received TMS during the delay phase. In a separate group of participants performing the same task, conditioning spTMS was applied to the ventral premotor cortex (vPM) 7 ms before test spTMS. Results showed that conditioning TMS over OP modulated M1 output according to the information on object size that had been acquired haptically but not visually. Vice versa, conditioning TMS over vPM modulated M1 output according to information on object size acquired by vision but not haptically. Moreover spTMS over OP produced a significant modulation of the upcoming reaching behavior only when the object had been explored haptically. We show that OP contains a haptic memory of objects' macrogeometry and the appropriate motor plan for grasping them.

Keywords: premotor cortex, sensorimotor transformation, tactile memory, transcranial magnetic stimulation, working memory

Introduction

The human parietal operculum (OP) is a heterogeneous cortical region located above the caudal Silvian fissure comprising Brodmann's areas 39, 40, 43, 3, 1, and 2 (Eickhoff et al. 2006a, 2006b). It embeds 2 complete tactile sensory representations of the body and is considered an important station for processing somatosensory information (Krubitzer and Kaas 1990; Krubitzer et al. 1995). OP neurons respond to non-noxious and noxious cutaneous and muscular stimuli and to proprioceptive inputs generated by passive joint movements, in nonhuman (Krubitzer et al. 1995; Fitzgerald et al. 2006) and human (Woolsey et al. 1979; Treede and Kunde 1995; Svensson et al. 1997; Disbrow et al. 2000; Del Gratta et al. 2002; Mazzola et al. 2012) primates. The portion of OP that contains such somatosensory representation is historically referred to as the secondary somatosensory cortex (SII). Parts of OP are also recruited during active movements. This activity has been considered the consequence of the proprioceptive reafference caused by movement (Faillenot et al. 1997; Binkofski et al. 1999a; 1999b; Ehrsson et al. 2000; 2003), but it also suggests a direct role of OP in the coordination of movement (Jancke et al. 2001; Reed et al. 2004). Dual coil transcranial magnetic stimulation (TMS), also referred to as twin-coil TMS or bifocal TMS, is a powerful method to probe the functional link between cortical areas (Koch et al. 2007; O'Shea et al. 2007; Davare et al. 2009). In a recent article, we mapped the connectivity of the entire hemisphere with the ipsilateral M1 by means of a dual coil paradigm in subjects at rest (Cattaneo and Barchiesi 2011). Among other results, we observed that TMS applied to the OP produced a short-latency effect on M1, supporting the presence of direct cortico-cortical connections between the 2 regions. These findings indicate that some OP neurons are just one synapse away from the motor cortex (M1) and are in agreement with anatomical studies in nonhuman primates. Indeed, a substantial proportion of M1 neurons is stained following the injection of anterograde tracers in monkey OP (Mesulam and Mufson 1982; Mufson and Mesulam 1982; Pandya and Seltzer 1982; Cusick et al. 1989; Krubitzer and Kaas 1990; Stepniewska et al. 1993; Cipolloni and Pandya 1999; Qi et al. 2002; Disbrow et al. 2003). What could be the role of such connections? A plausible hypothesis is that OP is involved in the direct transformation of somatosensory information in motor commands. In favor of such hypothesis, a recent re-classification of cytoarchitectonic parcellation of the OP region in humans has indicated that its dorso-rostral portion (labeled OP4) is characterized by its connections to M1 and is probably separated from the classically defined the secondary somatosensory area (Eickhoff et al. 2010). In the present work, we investigated the possibility that OP plays a direct role in haptically guided grasping by means of dual-coil TMS. Test stimuli (*testTMS*) were applied to M1 and conditioning TMS (*condTMS)* to the ipsilateral OP at short interstimulus intervals (ISIs). At first, we studied in baseline conditions the optimal stimulation point in the OP cortex and the optimal ISIs for eliciting short-latency modulation of M1 (Experiment 1). In the main experiment (Experiment 2), OP-M1 connectivity was tested while participants were preparing the blindfolded grasp of an object, the variable size of which had been previously explored by the participant in the haptic or in the visual modality. Finally, in a complementary experiment (included in Experiment 2), we controlled for the validity of the effects of OP stimulation by implementing the same experimental paradigm with stimulation of the ventral premotor cortex (vPM), which is well known to play a role in visually rather than haptically guided grasping.

Materials and Methods

Participants

Five right-handed volunteers took part in Experiment 1 (3 females, age 25.6 ± 2.8 years). Twenty-four right-handed volunteers participated in Experiment 2 (14 females aged 32.2 ± 3.6 years) and were split in 2 groups. Twelve participants received *condTMS* over the left OP region (referred to as "OP group"), whereas the other 12 received *condTMS* over the left vPM region (referred to as "vPM group"). None of them had contraindications to TMS (Rossi et al. 2009) and all gave written informed consent in accordance with the Ethical Committee of the University of Trento (protocol n. 2009-033).

MRI and Neuronavigation

All MRI data were acquired with a 4T scanner (Bruker Medical, Ettlingen, Germany) using a birdcage transmit, 8-channel receiver head radiofrequency coil. Structural images were acquired using a 3D magnetization prepared rapid gradient echo sequence (3D MPRAGE) optimized for gray–white matter contrast [$1 \times 1 \times 1$ mm^3 resolution, echo time (TE) = 4.18 ms, repetition time (TR) = 2700 ms, inversion time (TI) = 1020 ms, flip angle = 7°, Generalized Autocalibrating Partially Parallel Acquisition acceleration factor = 2]. Anatomical images in Digital Imaging and Communications in Medicine format of each participant were then processed using the Brainvoyager software (Brain Innovation BV, The Netherlands) to produce a 3D surface reconstruction of the scalp and of the gray matter surface. The opercular subregion that we aimed to cover with the grid was the OP4 part, defined according to (Eickhoff et al. 2006a). We obtained the OP4 mask from the Statistical Parametric Mapping (SPM5) anatomy toolbox (Wellcome Department of Cognitive Neurology; http://www.fil.ion.ucl.ac.uk/spm) implemented in Matlab 2007 (Mathworks, Inc.) in the Neuroimaging Informatics Technology Initiative (NIfTI-1) format. Such mask was then converted in Brainvoyager-compatible format using the NIfTI converter plugin for Brainvoyager QX (available at http://support.brainvoyager.com). The participant's head and the *condTMS* coil were co-registered with the scalp 3D reconstruction by means of the Neuronavigation module of the Brainvoyager software, interfaced with the ultrasound tracker CMS20S (Zebris Medical, Isny, Germany). This allowed online updating of the position of the *condTMS* coil over the scalp.

Dual Coil TMS

The stimulation paradigm used was the same as in Cattaneo and Barchiesi (2011). Two different magnetic stimulators, each connected to a separate coil were used simultaneously. A Magstim 200 monophasic stimulator (The Magstim Company, Whitland, UK) was used to deliver the *testTMS* via a Magstim custom-made figure-of-eight coil with 50-mm-diameter windings. A Magpro stimulator (Magventure, Skovlunde, Denmark) in biphasic stimulus modality produced the *condTMS* via an MC-B35 coil with winding diameter of 36 mm. The participants' heads were held still with a chin-rest incorporating an additional lateral head-constrain.

The *testTMS* coil was permanently positioned on hand motor cortex of the left-hemisphere and held in place by means of a mechanical support. It was oriented with the handle pointing medially forming a 90° angle with the midline. The optimal coil orientation for transsynaptic stimulation of corticospinal neurons in the hand representation in M1 is known to be of 45° (Mills et al. 1992). In our protocol however, in order to allow the concurrent presence of the 2 coils on the scalp surface, we adopted the configuration described above. Besides, other studies have shown that also a current orientation perpendicular to the midline elicits preferentially indirect waves in the cortico-spinal descending volley (Sakai et al. 1997). *TestTMS* was delivered at an intensity corresponding to 120% of individual resting motor threshold (Rossini et al. 1994) calculated for the right "interosseus dorsalis primus" (ID1) muscle.

Electromyographic Recordings

Motor evoked potentials (MEPs) were recorded from the right ID1 muscle in Experiment 1 and from the ID1 and the "extensor indicis proprius" (EIP) muscles in Experiment 2. The ID1 muscle originates from the base of the first and second metacarpal bones and inserts on the proximal phalanx of the index finger. Its action is therefore that of abducting and flexing the index finger around the metacarpophalangeal joint. The EIP muscle arises from the distal third of the ulna and by intermediation of the dorsal aponeurosis, it acts upon the distal phalanx of the index. Its action is therefore that of extending the whole index finger. These 2 muscles therefore can act as antagonists in flexion-extension movements of the index finger, as in the experimental task adopted in Experiment 2. It should however be made clear that the 2 muscles are not obligatory antagonists because they can be partially synergistic in the abduction of the index finger (Brochier et al. 2004).

Recordings were realized by means of passive Ag/AgCl electrodes in a bipolar belly-tendon montage. The analog Electromyographic (EMG) signal was then amplified 1000× by means of a CED 1902 amplifier (Cambridge Electronic Design, Cambridge, UK) and digitized by means of a CED 1401 micro Mk-II unit (Cambridge Electronic Design, Cambridge, UK) at a sampling frequency of 4 KHz. In Experiment 1, the EMG recording was triggered by the *testTMS* pulse (time = 0.0) by means of the Signal software (Cambridge Electronic Design, Cambridge, UK). In each trial, EMG was recorded from −250 to +250 ms and stored on a PC for offline analysis. In Experiment 2, a continuous recording of the EMG activity was carried out throughout the whole experiment by means of the Spike II software. Peak–peak amplitudes of MEPs were extracted by an automatic algorithm in the Signal software seeking for the maximum and minimum EMG values in a time window from 20 to 40 ms after *testTMS*.

Experiment 1: General Design

The first experiment aimed at establishing the optimal position and ISI to produce short-latency effects by *condTMS* to M1. To do so, we tested participants while sitting at rest and moved the *condTMS* coil over a grid of scalp points that covered the whole of the OP region. Moreover we tested different ISIs between condTMS and testTMS. The analysis of the data was first carried out on a single-subject basis by computing statistical scalp maps of the comparison between *condTMS* + *testTMS* trials with *testTMS* trials. Finally, a group analysis was carried out to generalize the findings from single subjects.

Experiment 1: Mapping Procedure

We built in each participant a 3×3 grid drawn over the left OP region (Fig. 1 shows individual grids in the 5 participants). The *condTMS* coil was moved sequentially over the grid-points under online neuronavigation guidance and its intensity was set at 90% of resting motor threshold computed for ID1. Three different ISIs were used (5, 7, and 9 ms) in a separate blocks. The mapping procedure consisted in a sequence of *condTMS* + *testTMS* trials following a fixed spatial order over the grid. The moment of TMS was manually determined in each trial by the operator whenever the *condTMS* coil had been moved over the following point of the grid.

All 9 points of the grid were therefore tested at every cycle of 9 consecutive *condTMS* + *testTMS*. This cycle was repeated 16 times in order to have 16 repeated measures of *condTMS* + *testTMS* for each grid point. Trials with only *testTMS* were interleaved in the mapping sequence every 3 *condTMS* + *testTMS* trials. The session of stimulation described was repeated for 3 blocks, each with a different ISI. To summarize, each of the 3 blocks was composed by 144 (9 points × 16 repetitions) *condTMS* + *testTMS* trials interleaved with 48 tTMS-only trials for a total of 192 trials.

Conditioned TMS paradigms conventionally use the grand average of test MEP amplitudes from the whole block as the denominator of the normalization ratio (e.g., see Kujirai et al. (1993) or Ziemann et al. (1998b)). In the present work, we performed lengthy experimental sessions in which the test MEP amplitude was likely to vary greatly in the course of the block for spontaneous fluctuations of vigilance or for technical aspects such as coil heating and switching. We therefore decided to adopt a quasi-instantaneous measure of test MEP amplitudes represented by the average of 2 adjacent *testTMS* trials moving along the timeline of the block in a sliding window, as described in (Cattaneo and Barchiesi 2011). Therefore each MEP from *condTMS* + *testTMS* trials was normalized to the mean of the 2 test MEPs preceding and following the conditioned trial.

Experiment 1: Computation of TMS Statistical Maps and Group Analysis

The data from each ISI was analyzed separately. As a result of MEP processing and normalization we obtained for each of the 3 ISIs a series of 16 normalized MEP amplitudes, each varying from 0 to +∞, for each of the 9 points composing the grid. Values >1 represented facilitatory effects of *condTMS* and values <1 represented inhibitory effects of *condTMS*. Such values were transformed logarithmically in order to

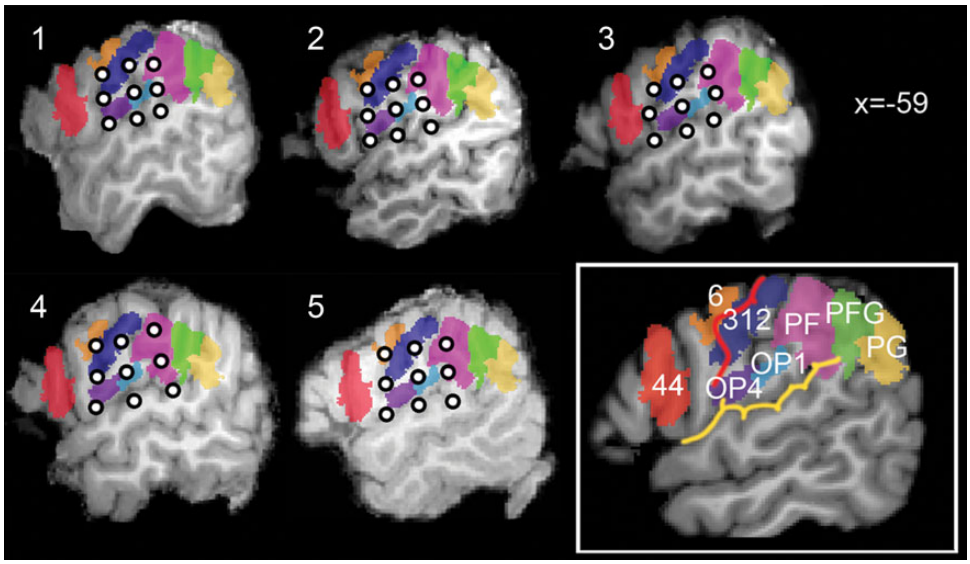

Figure 1. Individual MRI scans of the 5 participants to Experiment 1 at the sagittal section corresponding to $x = -59$. Superimposed over the MRI scans is the probabilistic (50% probability) cytoarchitectonic maps and the projection from the scalp of the individual 9-point grids. The lower-right panel shows on a standard brain the labels of the cytoarchitectonic areas. The central sulcus is indicated in red and the Silvian fissure in yellow.

obtain a distribution of the data varying between $-\infty$ and $+\infty$. After this process, values >0 represented facilitatory effects of *condTMS* and values <0 represented inhibitory effects of *condTMS*. At last, each of the 9 distributions of 16 data was analyzed in a 2-tailed *t*-test for single samples, against the null hypothesis that the distribution had a mean value of zero. Significance level for the *t*-test was corrected for the 9 comparisons within the grid and therefore was set to $P = 0.05/9 = 0.0056$. In order to quantify the distribution of the effects of *condTMS* at the group level, we performed an ANOVA on *t*-values with 2 factors: ISI (3 levels: 5, 7, and 9 ms) and POINT (9 levels corresponding to the 9 grid points).

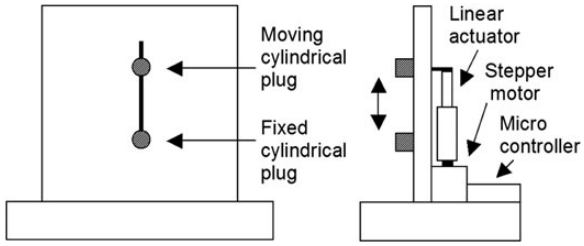

Figure 2. Schematics of the apparatus controlling interplug distance.

Experiment 2: General Design and Experimental Setup

Participants were tested in dynamic conditions during a delayed reach and grasp task. They were divided in 2 groups according to whether they received *condTMS* over the OP or over the vPM. In both groups, *condTMS* intensity was set at 90% of resting motor threshold computed for right ID1. The *condTMS* coil was positioned following the neuronavigation system on one single spot for every participant. In the OP group, *condTMS* was applied to a single point in the OP region that was established on the basis of the maps obtained in Experiment 1, as a point along the postcentral sulcus, 2 cm above the Silvian fissure. In the vPM group, the target of *condTMS* was established on the basis of previous dual-coil TMS experiments for the study of vPM-M1 interactions (Baumer et al. 2009; Davare et al. 2009, 2010; Koch et al. 2010; Lago et al. 2010) as a point along the precentral sulcus, 1.5 cm below the intersection with the inferior frontal sulcus. In this experiment, also the ISI between *condTMS* and *testTMS* was fixed and corresponded to 5 ms for the OP group, which was defined as the optimal ISI in Experiment 1 and to 7 ms in the vPM group (Davare et al. 2009).

Subjects were sitting on a comfortable chair with their head placed in the chin rest. A custom-made (www.lmelettronica.it) apparatus holding 2 plastic plugs (Fig. 2) was placed in front of them. The distance between the plugs was varied randomly at every trial. The lower plug was fixed to a vertical panel, the upper plug moved inside a vertical fissure in the panel, by virtue of a linear actuator connected to a stepper motor in the rear part of the panel. The whole automation was implemented by using an ArduinoUNO microcontroller (www.arduino.cc) which generated at each trial a random number that was converted in interplug distance. A linear potentiometer connected to the plugs assured feedback to the microcontroller on the interplug distance. The setup consisted additionally in (A) a switch on the table on which the participant's right hand rested and which signaled the start of the Reach phase. (B) A small touch-sensitive sensor placed over the upper plug in order to signal the time of contact of the hand with the object. (C) A pair of computer-controlled liquid crystal shutter goggles (Plato Translucent Technologies, Inc.) worn by subjects in the whole experiment. Additionally, participants were wearing earphones in order to hear acoustic cue-sounds and white noise played in the background. The participant's left hand was kept in a rest condition for the whole experimental session.

Experiment 2: Trial Structure and Order

The participant's task is schematized in Figure 3 and consisted in a Rest phase, followed by exploration of the interplug distance, either visually or haptically, followed by a Delay phase in which participants waited for TMS. The TMS pulse served as the GO-signal and instructed the participants to release the home switch to reach and grasp the plugs with their index and thumb fingertips. TMS was therefore delivered when the participant had already acquired the information on the interplug distance to be grasped, and was waiting to use that information to perform the grasp.

Visual and haptic trials were identical in the Rest, Delay, and Grasp phases but differed in the Exploration phase. At the beginning of each trial, subjects were sitting with vision occluded by the shut goggles and with their right hand relaxed on the home switch while the distance between the 2 objects was being changed. In the subsequent exploration phase, the shutter lenses were opened for 2000 ms in order to allow vision of the objects in Visual Exploration. Goggles instead remained closed in haptic trials and an acoustic cue-sound prompted the subjects to start tactile exploration of the plugs with their right hand.

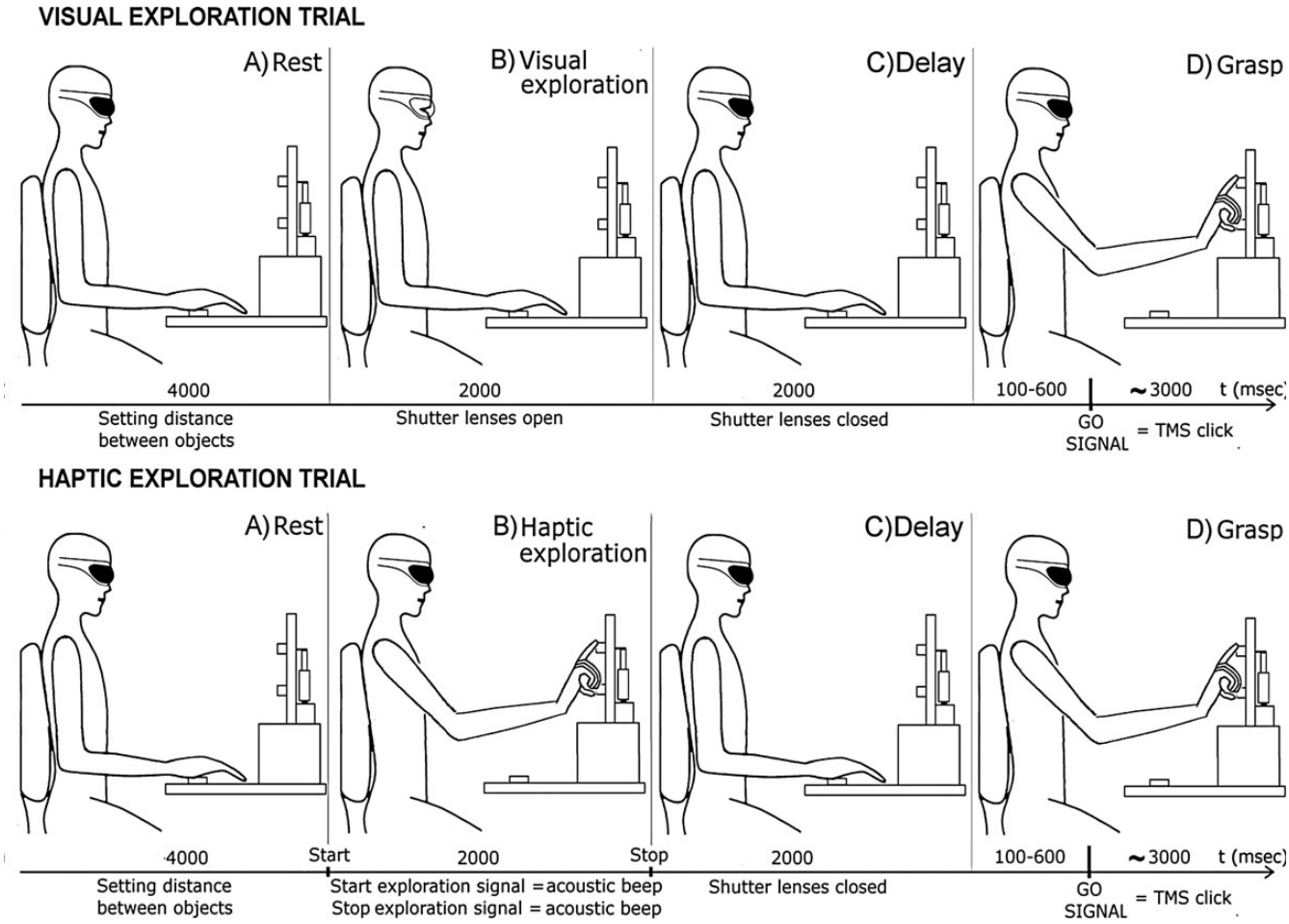

Figure 3. Top: Visual exploration trial. Bottom: Haptic exploration trial. Each trial is composed by 4 phases: (*A*) Rest, change of interplug distance; (*B*) Exploration: visual or haptic according with the type of trial (note that in haptic trials the vision of the object was occluded in this phase); (*C*) Set: the subject waits for the GO-signal; (*D*) Reach-grasp: the participant, with vision occluded in both trial types, performs a thumb-index grasping of the 2 plugs.

After 2000 ms, another acoustic cue advised participant to finish the exploration and go back to the rest position. During this Delay phase, subjects were instructed to be ready to perform a thumb-index grasp of the plugs whenever they heard the GO signal. The GO signal occurred randomly between 2100 and 2600 ms after the end of the visual or haptic inspection. Once the plugs were grasped, subjects returned with their right hand relaxed on the home switch.

The interplug distance was fully randomized between trials, the order of trials was fixed in the sequence: 1) Visual Exploration trial with *cond* + *testTMS*, 2) Visual Exploration trial with *testTMS* alone, 3) Haptic Exploration trial with *cond* + *testTMS*, 4) Haptic Exploration trial with *testTMS* alone. This basic sequence was repeated 50 times for a total duration of the experimental session of 35 min. For each trial, the set interplug distance and the timing of the go signal (TMS) were recorded in a log file by the Arduino system. The number of trials was 200 per each experimental session corresponding to 50 trials per each of the 4 conditions: 1) single pulse-visual trial, 2) single pulse-haptic trial, 3) dual pulse-visual trial, and 4) dual-pulse-haptic trial.

Experiment 2: MEP Data Analysis

The strategy of data analysis in Experiment 2 was different from the conventional one used in Experiment 1. We did not compute the ratio between conditioned and test MEPs but focused on the modulation of raw MEP peak-to-peak amplitudes for each muscle. In each single subject, we calculated an index of correlation (Pearson's *r* coefficient) between the amplitude of MEPs obtained in single trials and the interplug distance of that same trial. The use of a statistical metric to describe the effect of an experimental factor and a physiological process is widely accepted and validated in functional neuroimaging studies (for more details, see Friston et al. 1991, 1995; Friston 1995). In our work, we decided to adopt this approach, and considered in our analysis the mutual combination of *r*-correlation coefficients between MEPs of the 2 antagonist muscles and the size of the grasped object. More precisely, we correlated MEP amplitudes with target size separately per each of the 4 conditions: 1) single pulse-visual trials, 2) single pulse-haptic trials, 3) dual pulse-visual trials, and 4) dual pulse-haptic trials. Each *r* value was computed on 50 pairs of data.

In our opinion, the use of a statistical parameter to describe the distribution of single trial measures (MEP amplitudes) according to an experimental variable (the target size) is more reliable than the conventional approach based on the extraction of mean values of MEP amplitudes in factorial designs. The main reason for this is that mean values of MEP amplitudes are strongly influenced by outlier data and that MEP amplitudes are not distributed normally, being comprised between 0 and $+\infty$. The use of correlation coefficients linking the dependent variable and the dimension that is manipulated experimentally overcomes this potential source of noise and bias. Correlation coefficients were calculated in single participants and take account therefore of values form each single trial. They were computed separately for each of the 2 muscles, thus resulting in 8 *r* values for each subject, corresponding to a 2*2*2 design with the factors: MODALITY (2 levels: haptic or visual), PULSE (2 levels: *testTMS* only or *condTMS* + *testTMS*) and MUSCLE (2 levels: ID1 and EIP). The *r* values have to be interpreted in 2 ways. First, their absolute values indicate that MEPs from a given muscle are correlated with the size of the object that has

been explored and that will be grasped. For each participant, positive and negative values of *r* indicate that the MEP size increases and decreases linearly with the size of the grasp target, respectively. Second, the 2 muscles are to be considered as mutual antagonists in the context of the present movement. Therefore, besides their absolute values, also the mutual relation of *r* values between the 2 muscles within each condition is informative because it indicates whether the MEP modulation reflects the actual reach-grasp EMG pattern, in which it is expected that *r* values for the EIP muscle are more positive than those from the ID1 muscle. The *r* values were used as dependent variable in an ANOVA with the 3 within-subjects factors MODALITY*PULSE*MUSCLE and a between-subjects factor, that is, the GROUP (2 levels: OP group and vPM group).

Experiment 2: Analysis of EMG During the Reach-Grasp Action

We also performed a direct analysis of the EMG activity of the actual reach-grasp movements performed in the last phase of the trial (Grasp phase), that is, when subjects had already explored the target size. The epoch of the reaching movement was identified on the continuous EMG recordings with respect to home-switch release and plug-contact. The reaching epoch from each trial was then divided in 10 decile time bins. Electrical muscular activity started slightly before the mechanical event of hand elevation and, obviously, continued after the contact with the target. Therefore, in each trial, we considered also 2 additional time bins immediately preceding and immediately following the reach, with duration identical to the deciles of that trial. This procedure resulted for each trial in a total of 12 consecutive time intervals of equal length. The average duration of deciles among trials and subjects was of 111 ms (SD: 12 ms). The rectified EMG activity was averaged in each 2 consecutive time bins, resulting in 6 values per trial corresponding to the time-course of EMG along the reaching movement. Pearson's *r* coefficient was computed between each of the 6 EMG values for the 2 muscles and the interplug distance of that trial. As with MEP analysis, the correlations were computed per each of the 4 conditions: 1) single pulse-visual trial, 2) single pulse-haptic trial, 3) dual pulse-visual trial, and 4) dual-pulse-haptic trial. Therefore, each *r* value was computed on 50 pairs of data. The EMG-target size correlations were then analyzed with an ANOVA with 4 within-subjects factors: TIME (6 levels corresponding to the 6 consecutive time bins), MODALITY (2 levels, visual or haptic), PULSE (2 levels, single or dual pulse), and MUSCLE (2 levels, ID1 and EPI) and 1 between-subjects factor, GROUP (2 levels, OP and vPM) as between-subjects factor.

Results

None of the participants reported either immediate or delayed side effects of TMS.

Experiment 1

The results of the mapping experiment showed the existence of a short-latency modulation of *condTMS* delivered over OP on corticospinal excitability which is both temporally and spatially specific. The single-sample *t*-test performed on the points of individual grids produced significant results in all 5 subjects only at the ISI of 5 ms. The location of significant spots was distributed along the mid portion of the grid. All significant effects were inhibitory (Fig. 4 upper panel). The ANOVA with GRID POINT and ISI as within-subjects factors showed that a significant distribution of *t*-values was present only for the 5 ms ISI. The ANOVA also showed that at the group level, a significant effect of *condTMS* was observed only for the grid point p5 (Bonferroni-corrected $P = 0.02$) (Figure 4 lower panel). This corresponded to the ventral part of the postcentral sulcus, at the border between the OP4 and the OP1 region.

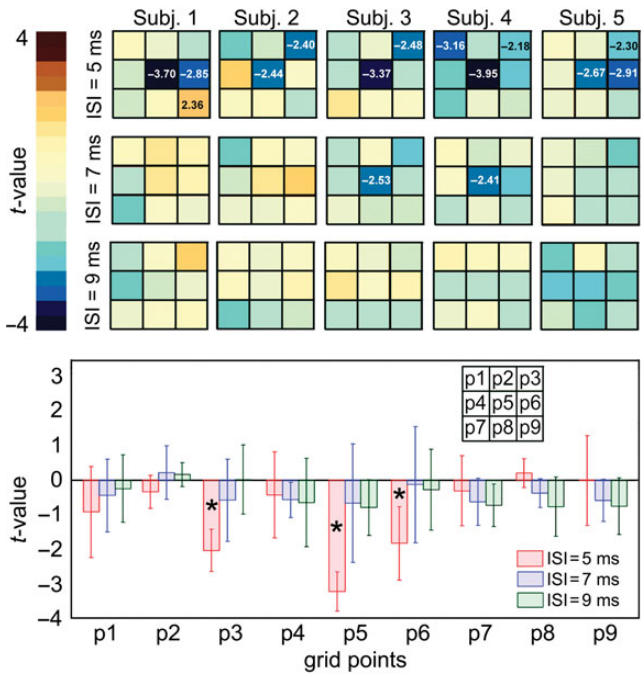

Figure 4. Upper panel: individual statistical maps of the *t*-values obtained contrasting the distribution of log(condMEP + testMEP/testMEP) against the null hypothesis of the mean value = 0. Values of *t* are reported when they exceeded 2.13, that is, the one corresponding to a *P*-value of $P = 0.05$ at 15 degrees of freedom. The *t*-value Bonferroni corrected for 9 multiple comparisons ($P = 0.0056$) corresponded to 3.25. Lower panel: mean *t*-values from all 5 participants. Asterisks indicate the grid points with significant differences of the mean values from chance level ($t = 0$). The inserted grid indicates the nomenclature of the grid points. Note that orientation conventions of the grids are to be interpreted as overlying the scalp of the left hemisphere; therefore, they are oriented with the cranial direction to the left and the caudal direction to the right.

Experiment 2: Correlations Between MEPs and Target Size

The results of the ANOVA performed on *r* coefficients obtained from the MEP amplitudes produced a significant main effect of MUSCLE ($F(1, 22) = 7.99$, $P = 0.01$) driven by the lower values of *r* coefficients associated with the ID1 muscle compared with those associated to the EIP muscle. The most important finding however was a 4-way GROUP*MODALITY*PULSE*-MUSCLE interaction ($F(1, 22) = 19.78$, $P = 0.0002$) which is illustrated in Figure 5. To explore the complex interaction we divided the analysis between the 2 groups in 2 symmetrical MODALITY*PULSE*MUSCLE ANOVAs, which both resulted in significant 3-way interactions ($F(1, 11) = 15.34$, $P = 0.002$ in the OP group and $F(1, 11) = 8.18$, $P = 0.016$ in the vPM group). We broke each interaction effect into 2 PULSE* MUSCLE sub-ANOVAs for each of the 2 sensory modalities. The results in the OP group showed a significant PULSE*MUSCLE interaction for the tactile modality ($F(1, 11) = 23.03$, $P = 0.0006$) but no interaction in the visual modality ($F(1, 11) = 0.05$, $P = 0.83$). Post hoc *t*-tests indicated that the interaction was to be attributed to the fact that no difference was present between the *r* coefficients from the 2 muscles in the single pulse modality (Bonferroni-corrected $P = 1.0$), while a consistent difference was present between the mean *r* coefficients of the 2 muscles in the dual-pulse modality, that is, when also OP had been stimulated with TMS (Bonferroni-corrected $P = 0.00006$). On the contrary, the same analysis performed in the vPM group

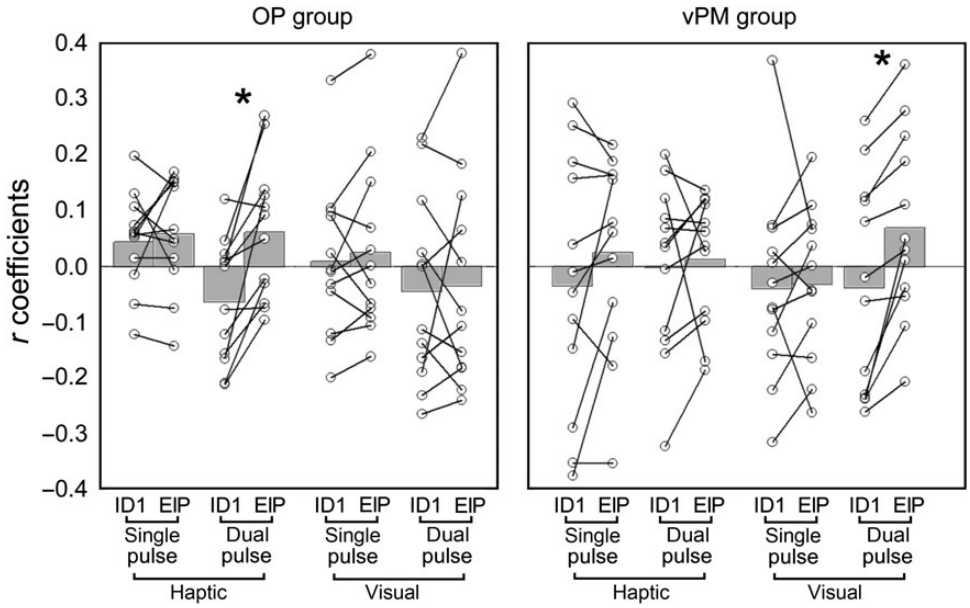

Figure 5. Grey columns indicate the mean *r* coefficients calculated on the MEPs from the 2 muscles in the different experimental conditions. Line-circle elements indicate the individual data. The asterisks indicate the significant post hoc comparisons.

did not show any PULSE*MUSCLE interaction in the haptic modality ($F(1, 11) = 0.96$, $P = 0.35$) but did show a significant PULSE*MUSCLE interaction in the visual modality ($F(1, 11) = 6.71$, $P = 0.025$). Post hoc comparisons indicated that the interaction was ultimately due to a difference between *r* coefficients from the 2 muscles in the dual-pulse trials (Bonferroni-corrected $P = 0.022$) but not in the single-pulse trials (Bonferroni-corrected $P = 1.0$).

Additionally, as a post hoc analysis aimed at assessing whether any correlation was present between the MEPs in each category and the target size, we performed single-sample *t*-tests against the null hypothesis of mean $x = 0.0$. The results did not show any significant result (minimum $P = 0.08$).

Experiment 2: Effects of TMS on the Subsequent Reach-Grasp Movement

Figure 6 illustrates qualitatively in one representative subject the relation between the EMG recorded from the 2 muscles and the size of the object to be grasped. The results of the ANOVA showed a TIME*MUSCLE interaction ($F(5, 110) = 62.57$, $P < 0.000001$) which indicates the divergent time course of the *r* coefficients from the 2 muscles during the Reach-Grasp phase. As shown in Figure 7, the EIP muscle showed an activity that was correlated from very early in the reach with the geometry of the target object as indicated by the deviance from the 0 value (dashed line in Fig. 7). The ID1 muscle on the contrary is specifically activated in relation to the object only very late in the reach and maximally during the grasp.

The most complex result of the ANOVA was a GROUP*MODALITY*TIME*MUSCLE interaction ($F(5, 110) = 3.43$, $P = 0.006$) that is illustrated in Figure 8. This interaction was further analyzed by means of 6 separate GROUP*MODALITY*MUSCLE ANOVAs, which yielded a significant 3-way interaction only in the second time bin ($F(1, 22) = 7.10$, $P = 0.014$). A further decomposition of the analysis indicated that only in the OP group a significant MODALITY*MUSCLE ($F(1, 11) = 14.67$, $P = 0.003$) interaction was present. Post hoc comparisons

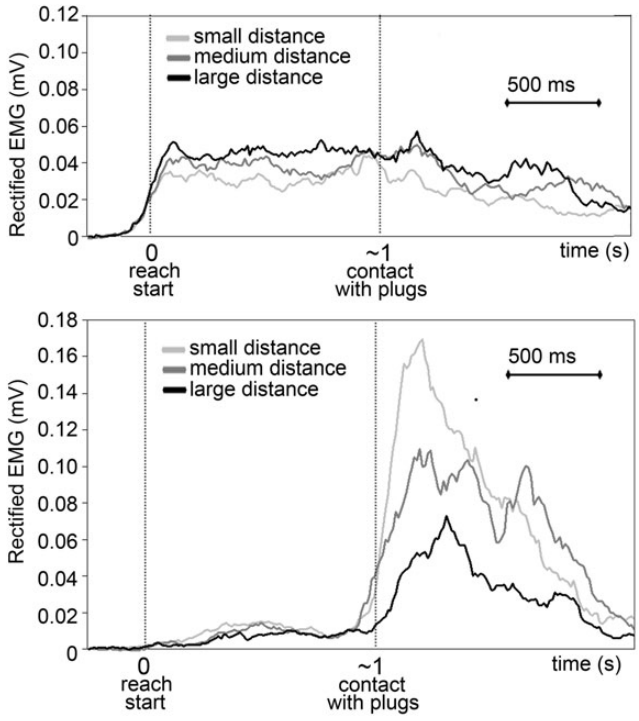

Figure 6. The rectified EMG recordings of the EIP and ID1 muscles from one representative subject are represented, to illustrate the relation of the EMG signal to the size of the object. The data from the single-pulse, haptic exploration condition are shown. For purely illustrative purposes, the EMG traces have been averaged in 3 groups, corresponding to the lower (small), middle (medium), and upper (large) thirds of interplug distances. All traces are aligned to the start of the reaching, that is, when the participant's hand was lifted from the start-switch. In this particular subject contact with the plugs occurred around 1 s later. Notice that EIP muscle activity increases with increasing interplug distance and conversely ID1 activity decreases with the size of the target.

indicated that the interaction was due to the fact that in the visual modality the mean *r* coefficients were significantly different between the 2 muscles (Bonferroni-corrected $P = 0.027$) but

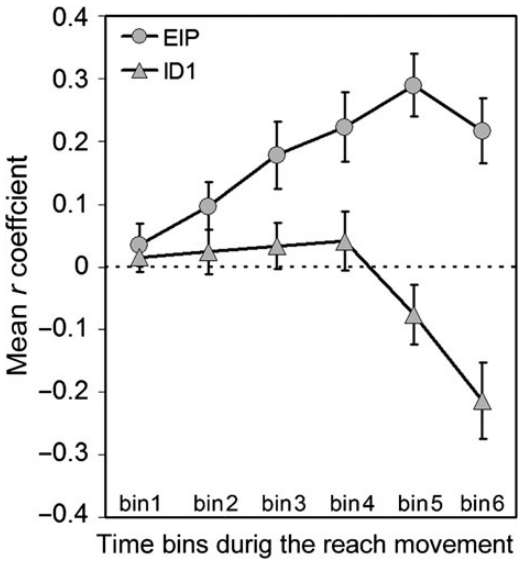

Figure 7. General time course of the *r* coefficients linking each of the 2 muscles with the interplug distance to be grasped. Bin 1 corresponds to the period around the GO-signal and bin 6 includes the contact with the plugs and the initial grasp phase. Bins 2–5 describe the reaching phase. The dashed line indicates $y = 0$. Error bars indicate 95% CI.

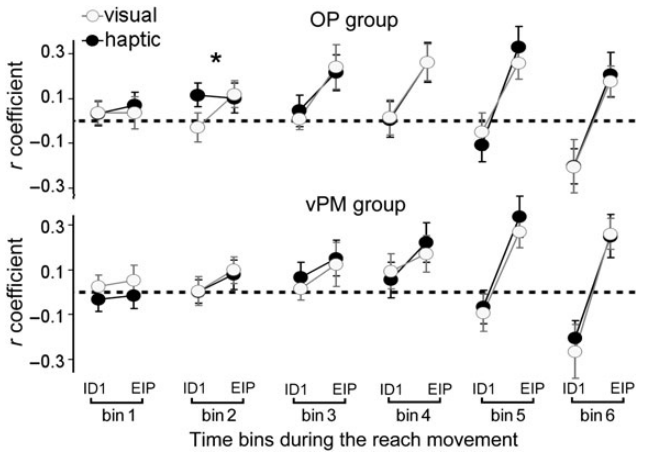

Figure 8. *r*-Coefficients resulting from the correlation of EMG values in the Reach-Grasp phase with the interplug distance. Error bars indicate 95% CI. The second bin, which resulted to be related to the 4-way interaction, is highlighted with an asterisk.

not so in the haptic modality (Bonferroni-corrected $P = 1.0$). Within the OP group, the results are not specific for the condition of dual pulse but are generally observed in the group of subjects who have been stimulated on the OP compared with those stimulated over the vPM.

Discussion

The results of Experiment 1, carried out on participants in the resting state, show that *condTMS* delivered on the OP produces a short-latency inhibitory effect on the representation of hand movements in M1. In dual coil paradigms the presence of short latency *condTMS-testTMS* interactions is attributed to either the presence of direct cortico-cortical connections between the 2 stimulated spots or to the convergence of corticospinal efferent projections from the 2 areas. In the case of the OP, both hypotheses are possible, because the OP region is known to be directly connected to M1 (Tokuno and Tanji 1993; Gharbawie et al. 2011a, 2011b) and to project fibres to the spinal cord (Galea and Darian-Smith 1994). In the present work, we did not control for changes at segmental level of motoneuron excitability produced by TMS of OP alone. We privilege the hypothesis that the short-latency modulation seen here is mainly due to cortico-cortical connections, considering the very small contribution of the OP to the corticospinal tract, that is, <3.5% of contralateral corticospinal projections in the macaque (Galea and Darian-Smith 1994).

In Experiment 1, the effects of *condTMS* show striking temporal and spatial specificity. The modulation effects of OP *condTMS* are specific to the ISI of 5 ms (Figure 4), consistent with a direct link between OP and M1. This datum is analogous to the well-established short-latency effects of premotor cortex stimulation on M1 neurons known in nonhuman primates (Tokuno and Nambu 2000; Kraskov et al. 2011) and humans (Davare et al. 2009) and it is likely that similar type of connections link OP to M1. We show that the conditioning effect is also restricted to a single small region along the postcentral sulcus. This spot corresponds to the caudal border of the OP4 region where direct projections to the primary motor cortex in human subjects are thought to arise (Eickhoff et al. 2006a, 2010). These results are also in agreement with anatomical evidence in macaque monkeys showing that the OP sends dense projections towards the hand representation of the premotor cortex and M1 (Tokuno and Tanji 1993; Gharbawie et al. 2011a). However, in TMS studies, the spatial relations between the stimulating coil and the underlying cortex is to be interpreted cautiously. The impact of TMS is likely to be maximum at sites different form that of the orthogonal projection of the centre of the coil onto the cortex and moreover it is not possible to assume that the effects of TMS are due to stimulation of a single cortical site but rather to the simultaneous activation of different though neighbouring patches of cortex (Thielscher and Wichmann 2009; Thielscher et al. 2010). In the present data, though we found that the most efficient coil position right over the postcentral sulcus, the actual cortical origin of the short-latency effect of *condTMS* could be on a vaster region of the OP.

Experiment 2 investigated the role in processing haptic information for grasping of the OP-M1 interactions that had been demonstrated in Experiment 1. Previous data indirectly indicate that the motor functions of OP could be at least in part related to haptic knowledge of graspable objects' geometry. In humans, neuroimaging studies show that SII is active in tasks requiring the memorization of textures or 3D shapes acquired haptically (Bonda et al. 1996; Kaas et al. 2013). In monkeys, single neurons in SII present a sustained activity when haptic information is memorized for the later performance of a discrimination task (Romo et al. 2002). Finally, one imaging study showed that SII is particularly active when monkeys must rely on haptic memory to perform a reach-to-grasp movement in the dark (Nelissen and Vanduffel 2011). Our experiment extends these observations by showing that OP stores haptic information on object shape that is then to be transferred to M1 once a reach-to-grasp plan is implemented. This is indicated by the critical finding that in trials with testTMS only, no information on a motor plan to grasp that particular object size

could be extracted from the MEPs, ultimately suggesting that such information was not yet present in M1 at the time of TMS pulse.

This conclusion arises mainly from the mutual comparison of the *r* coefficients between the 2 muscles, rather than from a significant deviation of *r* coefficients in any of the conditions from the 0 value. In the first part of Experiment 2 we applied *condTMS* to the OP region. Prior to the actual movement, the pattern of conditioned corticospinal output from M1 to the EIP muscle was differently correlated with the interplug distance compared with the ID1 muscle pattern. More specifically, the EIP *r* coefficients were higher than those from the ID1 muscle. This result is in keeping with the fact that we recorded 2 muscles that are partially antagonists when actually producing the hand shape required in the task. The EIP is more active when reaching for the manipulandum with a large interplug distance than with a small interplug distance. Vice versa, the ID1 muscle needs to be more relaxed when reaching for large interplug distances than when reaching for small interplug distances (Figure 6). The reciprocal activity in the 2 muscles is therefore a signature of the variations of interplug distance as confirmed by analysing the ongoing EMG activity during the actual reach-grasp (Figure 7). Therefore, the significant PULSE*MUSCLE interaction following *condTMS* to the OP region can be explained exclusively by hypothesizing that muscle-specific information to be used for reaching-grasping is present in OP and is readily transferable to M1. These interactions are functionally relevant only when information relative to object geometry is acquired haptically but not visually (Figure 5).

In the second part of the experiment, we applied *condTMS* to vPM to a second group of participants. Taken together with the results of the OP group of participants, the data show a clear double dissociation between sensory modality and stimulated cortical area. Indeed, in the vPM group, we found that the conditioned corticospinal output was predictive of the motor plan required to grasp an object of a given geometry only when that information was acquired visually and not haptically. The results in the vPM group are consistent with the effects characterizing PMv–MI interaction in the visual modality previously reported (Davare et al. 2009). Altogether, these results show that SII and PMv are 2 essential components of the cortical grasping network in which they support highly complementary functions. It is likely that direct connections between these 2 areas are required to coordinate their activity and their interaction with M1 during grasp. As stated above while discussing the results of Experiment 1, the effects of the conditioning TMS on corticospinal excitability are likely to reflect cortico-cortical interactions. Differently from what observed in Experiment 1, the net effects of *condTMS* are not merely inhibitory, but rather modulate the net output of M1 in the corticospinal system in a task-dependent pattern. As shown in previous twin-coil bifocal TMS studies and reviewed by (Koch and Rothwell 2009), the effects of conditioning TMS cannot be possibly classified as simply inhibitory or excitatory, but rather instantaneously indicate the transfer of information within a cortical network.

The task used in the present experiment actually tests the capacity of the brain to hold in a working memory system the motor plan required to grasp an object of a given geometry. Some observations on this should be made. The issue of the neural site of tactile working memory for objects is not well defined because most studies focused on the retention of memory of textures rather than macro-geometrical object features. There is general agreement on the fact that haptic memory is supported by an expert and dedicated system which resides probably in a ventral network passing from the somatosensory cortex, the OP and insula, and, finally, the frontal cortex as reviewed in (Burton and Sinclair 2000; Pasternak and Greenlee 2005). Although our task was based on memory retention of object geometry, our data also suggest that OP plays a key function during grasping by transferring information to be used for movement to M1 (Milner et al. 2007). From a further perspective, perception-action coupling theories generally are aimed at identifying several hierarchical levels of sensorimotor interactions, as reviewed by Lebedev and Wise (2002), but do not take into account the possible differences between sensory modalities. In fact, most models on perception-action coupling indicate the premotor cortex as a pivotal node from which all information needs to pass to be transformed into movement. Our data suggest that the premotor cortex does not cover this role for all sensory modalities. Haptically guided behavior relies on a distinct network in which the role of the OP is that of a "premotor" cortex where the term premotor does not refer to anatomy, but rather to its functional position in the circuit.

In addition, we provide unprecedented indications that the OP region is "causally" involved in the use of haptic information for the reaching-grasping movements. We analyzed the actual pattern of ongoing EMG activity while subjects were reaching for the manipulandum and its correlation with object size (Figure 8). We found in the very early phases of hand preshaping in the haptic task a significant difference in EMG activity between the OP and the vPM groups. More specifically, the physiological differentiation of EMG activity between the 2 recorded muscles (namely, higher *r* values for EIP than those for ID1 muscle) occurred later in the OP group compared with the vPM group. We did not find a significant effect of the PULSE factor.

Our interpretation of this datum is that repeatedly targeting OP with spTMS produced a cumulative effect that was observed throughout the experimental session. The statistical results indicate that this sort of after-effect was present in both trials with only *testTMS* over M1 and in the ones with also *condTMS* over OP. Given the invariance of all other experimental conditions, including the sensory modality, the difference between the 2 groups can only be attributed to the site of application of *condTMS*. But how is it possible that it is evident also for *testTMS*-only trials? The observed changes in performance could be due to cumulative effects of TMS applied to OP along the whole experimental session. In other words, this would be a repetitive TMS-like effect, resulting ultimately in a change in motor performance during the actual reaching for the object. In a post hoc analysis we observed that the frequency of stimulation of OP was of 0.05 Hz. This is beyond 0.1 Hz that is considered the limit for carry-over effects of simple rTMS (Chen et al. 1997). However, in the absence of any other better explanation, we hypothesize that the particular patterned repetitive stimulation resulting from the ordered sequence of trials applied here might escape the conventions established for simple frequency rTMS as has been shown, for example, for 0.1 Hz TMS coupled with peripheral deafferentation (Ziemann et al. 1998a). In the absence of a baseline condition (i.e., a condition without TMS), the interpretation of this

finding is not univocal because the possibility exists that the difference between the 2 groups is due to the vPM stimulation. Given that vPM *condTMS* did not produce any modulation of MEPs in the haptic modality while OP *condTMS* did, this seems a less likely possibility.

In summary, the present study indicates that OP and vPM play a fundamental role in the transformation of short-term memory of object geometry into a coherent pattern of muscle activation for grasping. Each of the 2 areas is specialized for one sensory modality, the OP contains information acquired haptically and the vPM contains visual information. Despite this segregation, the role of the 2 cortical stations appears very similar in storing macroscopic sensory information to be used in an open-loop manner for object-directed motor behavior.

Funding

The present work has been made also thanks to financial support from the Provincia Autonoma di Trento and Fondazione Cassa di Risparmio di Trento e Rovereto.

Notes

Conflict of Interest: None declared.

References

Baumer T, Schippling S, Kroeger J, Zittel S, Koch G, Thomalla G, Rothwell JC, Siebner HR, Orth M, Munchau A. 2009. Inhibitory and facilitatory connectivity from ventral premotor to primary motor cortex in healthy humans at rest—a bifocal TMS study. Clin Neurophysiol. 120:1724–1731.

Binkofski F, Buccino G, Posse S, Seitz RJ, Rizzolatti G, Freund H. 1999a. A fronto-parietal circuit for object manipulation in man: evidence from an fMRI-study. Eur J Neurosci. 11:3276–3286.

Binkofski F, Buccino G, Stephan KM, Rizzolatti G, Seitz RJ, Freund HJ. 1999b. A parieto-premotor network for object manipulation: evidence from neuroimaging. Exp Brain Res. 128:210–213.

Bonda E, Petrides M, Ostry D, Evans A. 1996. Specific involvement of human parietal systems and the amygdala in the perception of biological motion. J Neurosci. 16:3737–3744.

Brochier T, Spinks RL, Umilta MA, Lemon RN. 2004. Patterns of muscle activity underlying object-specific grasp by the macaque monkey. J Neurophysiol. 92:1770–1782.

Burton H, Sinclair RJ. 2000. Attending to and remembering tactile stimuli: a review of brain imaging data and single-neuron responses. J Clin Neurophysiol. 17:575–591.

Cattaneo L, Barchiesi G. 2011. Transcranial magnetic mapping of the short-latency modulations of corticospinal activity from the ipsilateral hemisphere during rest. Front Neural Circuits. 5:14.

Chen R, Classen J, Gerloff C, Celnik P, Wassermann EM, Hallett M, Cohen LG. 1997. Depression of motor cortex excitability by low-frequency transcranial magnetic stimulation. Neurology. 48: 1398–1403.

Cipolloni PB, Pandya DN. 1999. Cortical connections of the frontoparietal opercular areas in the rhesus monkey. J Comp Neurol. 403:431–458.

Cusick CG, Wall JT, Felleman DJ, Kaas JH. 1989. Somatotopic organization of the lateral sulcus of owl monkeys: area 3b, S-II, and a ventral somatosensory area. J Comp Neurol. 282:169–190.

Davare M, Montague K, Olivier E, Rothwell JC, Lemon RN. 2009. Ventral premotor to primary motor cortical interactions during object-driven grasp in humans. Cortex. 45:1050–1057.

Davare M, Rothwell JC, Lemon RN. 2010. Causal connectivity between the human anterior intraparietal area and premotor cortex during grasp. Curr Biol. 20:176–181.

Del Gratta C, Della Penna S, Ferretti A, Franciotti R, Pizzella V, Tartaro A, Torquati K, Bonomo L, Romani GL, Rossini PM. 2002. Topographic organization of the human primary and secondary somatosensory cortices: comparison of fMRI and MEG findings. Neuroimage. 17:1373–1383.

Disbrow E, Litinas E, Recanzone GH, Padberg J, Krubitzer L. 2003. Cortical connections of the second somatosensory area and the parietal ventral area in macaque monkeys. J Comp Neurol. 462:382–399.

Disbrow E, Roberts T, Krubitzer L. 2000. Somatotopic organization of cortical fields in the lateral sulcus of *Homo sapiens*: evidence for SII and PV. J Comp Neurol. 418:1–21.

Ehrsson HH, Fagergren A, Johansson RS, Forssberg H. 2003. Evidence for the involvement of the posterior parietal cortex in coordination of fingertip forces for grasp stability in manipulation. J Neurophysiol. 90:2978–2986.

Ehrsson HH, Fagergren A, Jonsson T, Westling G, Johansson RS, Forssberg H. 2000. Cortical activity in precision- versus power-grip tasks: an fMRI study. J Neurophysiol. 83:528–536.

Eickhoff SB, Amunts K, Mohlberg H, Zilles K. 2006a. The human parietal operculum. II. Stereotaxic maps and correlation with functional imaging results. Cereb Cortex. 16:268–279.

Eickhoff SB, Jbabdi S, Caspers S, Laird AR, Fox PT, Zilles K, Behrens TE. 2010. Anatomical and functional connectivity of cytoarchitectonic areas within the human parietal operculum. J Neurosci. 30:6409–6421.

Eickhoff SB, Schleicher A, Zilles K, Amunts K. 2006b. The human parietal operculum. I. Cytoarchitectonic mapping of subdivisions. Cereb Cortex. 16:254–267.

Faillenot I, Toni I, Decety J, Gregoire MC, Jeannerod M. 1997. Visual pathways for object-oriented action and object recognition: functional anatomy with PET. Cereb Cortex. 7:77–85.

Fitzgerald PJ, Lane JW, Thakur PH, Hsiao SS. 2006. Receptive field (RF) properties of the macaque second somatosensory cortex: RF size, shape, and somatotopic organization. J Neurosci. 26:6485–6495.

Friston KJ. 1995. Commentary and opinion: II. Statistical parametric mapping: ontology and current issues. J Cereb Blood Flow Metab. 15:361–370.

Friston KJ, Frith CD, Frackowiak RS, Turner R. 1995. Characterizing dynamic brain responses with fMRI: a multivariate approach. Neuroimage. 2:166–172.

Friston KJ, Frith CD, Liddle PF, Frackowiak RS. 1991. Comparing functional (PET) images: the assessment of significant change. J Cereb Blood Flow Metab. 11:690–699.

Galea MP, Darian-Smith I. 1994. Multiple corticospinal neuron populations in the macaque monkey are specified by their unique cortical origins, spinal terminations, and connections. Cereb Cortex. 4:166–194.

Gharbawie OA, Stepniewska I, Kaas JH. 2011a. Cortical connections of functional zones in posterior parietal cortex and frontal cortex motor regions in new world monkeys. Cereb Cortex. 21:1981–2002.

Gharbawie OA, Stepniewska I, Qi H, Kaas JH. 2011b. Multiple parietal-frontal pathways mediate grasping in macaque monkeys. J Neurosci. 31:11660–11677.

Jancke L, Kleinschmidt A, Mirzazade S, Shah NJ, Freund HJ. 2001. The role of the inferior parietal cortex in linking the tactile perception and manual construction of object shapes. Cereb Cortex. 11:114–121.

Kaas AL, van Mier H, Visser M, Goebel R. 2013. The neural substrate for working memory of tactile surface texture. Hum Brain Mapp. 34:1148–1162.

Koch G, Rothwell JC. 2009. TMS Investigations into the task-dependent functional interplay between human posterior parietal and motor cortex. Behav Brain Res. 202:147–152.

Koch G, Fernandez Del Olmo M, Cheeran B, Ruge D, Schippling S, Caltagirone C, Rothwell JC. 2007. Focal stimulation of the posterior parietal cortex increases the excitability of the ipsilateral motor cortex. J Neurosci. 27:6815–6822.

Koch G, Versace V, Bonni S, Lupo F, Gerfo EL, Oliveri M, Caltagirone C. 2010. Resonance of cortico-cortical connections of the motor system with the observation of goal directed grasping movements. Neuropsychologia.

Kraskov A, Prabhu G, Quallo MM, Lemon RN, Brochier T. 2011. Ventral premotor-motor cortex interactions in the macaque monkey during grasp: response of single neurons to intracortical microstimulation. J Neurosci. 31:8812–8821.
Krubitzer LA, Kaas JH. 1990. The organization and connections of somatosensory cortex in marmosets. J Neurosci. 10:952–974.
Krubitzer L, Clarey J, Tweedale R, Elston G, Calford M. 1995. A redefinition of somatosensory areas in the lateral sulcus of macaque monkeys. J Neurosci. 15:3821–3839.
Kujirai T, Caramia MD, Rothwell JC, Day BL, Thompson PD, Ferbert A, Wroe S, Asselman P, Marsden CD. 1993. Corticocortical inhibition in human motor cortex. J Physiol. 471:501–519.
Lago A, Koch G, Cheeran B, Marquez G, Sanchez JA, Ezquerro M, Giraldez M, Fernandez-del-Olmo M. 2010. Ventral premotor to primary motor cortical interactions during noxious and naturalistic action observation. Neuropsychologia. 48:1802–1806.
Lebedev MA, Wise SP. 2002. Insights into seeing and grasping: distinguishing the neural correlates of perception and action. Behav Cogn Neurosci Rev. 1:108–129.
Mazzola L, Faillenot I, Barral FG, Mauguiere F, Peyron R. 2012. Spatial segregation of somato-sensory and pain activations in the human operculo-insular cortex. Neuroimage. 60:409–418.
Mesulam MM, Mufson EJ. 1982. Insula of the old world monkey. III: efferent cortical output and comments on function. J Comp Neurol. 212:38–52.
Mills KR, Boniface SJ, Schubert M. 1992. Magnetic brain stimulation with a double coil: the importance of coil orientation. Electroencephalogr Clin Neurophysiol. 85:17–21.
Milner TE, Franklin DW, Imamizu H, Kawato M. 2007. Central control of grasp: manipulation of objects with complex and simple dynamics. Neuroimage. 36:388–395.
Mufson EJ, Mesulam MM. 1982. Insula of the old world monkey. II: afferent cortical input and comments on the claustrum. J Comp Neurol. 212:23–37.
Nelissen K, Vanduffel W. 2011. Grasping-related functional magnetic resonance imaging brain responses in the macaque monkey. J Neurosci. 31:8220–8229.
O'Shea J, Sebastian C, Boorman ED, Johansen-Berg H, Rushworth MF. 2007. Functional specificity of human premotor-motor cortical interactions during action selection. Eur J Neurosci. 26:2085–2095.
Pandya DN, Seltzer B. 1982. Intrinsic connections and architectonics of posterior parietal cortex in the rhesus monkey. J Comp Neurol. 204:196–210.
Pasternak T, Greenlee MW. 2005. Working memory in primate sensory systems. Nat Rev Neurosci. 6:97–107.
Qi HX, Lyon DC, Kaas JH. 2002. Cortical and thalamic connections of the parietal ventral somatosensory area in marmoset monkeys (Callithrix jacchus). J Comp Neurol. 443:168–182.
Reed CL, Shoham S, Halgren E. 2004. Neural substrates of tactile object recognition: an fMRI study. Hum Brain Mapp. 21:236–246.
Romo R, Hernandez A, Zainos A, Lemus L, Brody CD. 2002. Neuronal correlates of decision-making in secondary somatosensory cortex. Nat Neurosci. 5:1217–1225.
Rossi S, Hallett M, Rossini PM, Pascual-Leone A. 2009. Safety, ethical considerations, and application guidelines for the use of transcranial magnetic stimulation in clinical practice and research. Clin Neurophysiol. 120:2008–2039.
Rossini PM, Barker AT, Berardelli A, Caramia MD, Caruso G, Cracco RQ, Dimitrijevic MR, Hallett M, Katayama Y, Lucking CH et al.. 1994. Non-invasive electrical and magnetic stimulation of the brain, spinal cord and roots: basic principles and procedures for routine clinical application. Report of an IFCN committee. Electroencephalogr Clin Neurophysiol. 91:79–92.
Sakai K, Ugawa Y, Terao Y, Hanajima R, Furubayashi T, Kanazawa I. 1997. Preferential activation of different I waves by transcranial magnetic stimulation with a figure-of-eight-shaped coil. Exp Brain Res. 113:24–32.
Stepniewska I, Preuss TM, Kaas JH. 1993. Architectonics, somatotopic organization, and ipsilateral cortical connections of the primary motor area (M1) of owl monkeys. J Comp Neurol. 330:238–271.
Svensson P, Minoshima S, Beydoun A, Morrow TJ, Casey KL. 1997. Cerebral processing of acute skin and muscle pain in humans. J Neurophysiol. 78:450–460.
Thielscher A, Wichmann FA. 2009. Determining the cortical target of transcranial magnetic stimulation. Neuroimage. 47:1319–1330.
Thielscher A, Reichenbach A, Ugurbil K, Uludag K. 2010. The cortical site of visual suppression by transcranial magnetic stimulation. Cereb Cortex. 20:328–338.
Tokuno H, Nambu A. 2000. Organization of nonprimary motor cortical inputs on pyramidal and nonpyramidal tract neurons of primary motor cortex: An electrophysiological study in the macaque monkey. Cereb Cortex. 10:58–68.
Tokuno H, Tanji J. 1993. Input organization of distal and proximal forelimb areas in the monkey primary motor cortex: a retrograde double labeling study. J Comp Neurol. 333:199–209.
Treede RD, Kunde V. 1995. Middle-latency somatosensory evoked potentials after stimulation of the radial and median nerves: component structure and scalp topography. J Clin Neurophysiol. 12:291–301.
Woolsey CN, Erickson TC, Gilson WE. 1979. Localization in somatic sensory and motor areas of human cerebral cortex as determined by direct recording of evoked potentials and electrical stimulation. J Neurosurg. 51:476–506.
Ziemann U, Corwell B, Cohen LG. 1998a. Modulation of plasticity in human motor cortex after forearm ischemic nerve block. J Neurosci. 18:1115–1123.
Ziemann U, Tergau F, Wassermann EM, Wischer S, Hildebrandt J, Paulus W. 1998b. Demonstration of facilitatory I wave interaction in the human motor cortex by paired transcranial magnetic stimulation. J Physiol. 511(Pt 1):181–190.